Journal of Molecular Catalysis A: Chemical 339 (2011) 43–51

Contents lists available at ScienceDirect

Journal of Molecular Catalysis A: Chemical

journal homepage: www.elsevier.com/locate/molcata

XPS studies on the Cu(I,II)–polyampholyte heterogeneous catalyst: An insight into its structure and mechanism

Juan Manuel Lázaro Martínez[a], Enrique Rodríguez-Castellón[b,*], Rosa María Torres Sánchez[c], Lisandro Roberto Denaday[d], Graciela Yolanda Buldain[a], Viviana Campo Dall' Orto[d,**]

[a] Departamento de Química Orgánica, Facultad de Farmacia y Bioquímica, Universidad de Buenos Aires, Junín 956, Ciudad Autónoma de Buenos Aires (C1113AAD), Argentina
[b] Departamento de Química Inorgánica, Cristalografía y Mineralogía, Facultad de Ciencias, Universidad de Málaga, Campus de Teatinos, Málaga 29071, Spain
[c] CETMIC (Centro de Tecnología en Minerales y Cerámica) – Camino Centenario y 506, CC (49) (B1897ZCA) M. B. Gonnet, Argentina
[d] Departamento de Química Analítica y Fisicoquímica, Facultad de Farmacia y Bioquímica, Universidad de Buenos Aires, Junín 956, Ciudad Autónoma de Buenos Aires (C1113AAD), Argentina

ARTICLE INFO

Article history:
Received 29 July 2010
Received in revised form 14 January 2011
Accepted 22 February 2011
Available online 26 February 2011

Keywords:
Polyampholyte
Copper complex
XPS
Heterogeneous catalyst
Chlorinated phenols

ABSTRACT

A complex between Cu(II) and a polyampholyte synthesized from methacrylic acid, imidazole and ethyleneglycol diglycidyl ether was used as a heterogeneous catalyst for hydrogen peroxide activation and degradation of chlorophenols. The material was characterized by XPS and by measurements of the zeta potential. The isoelectric point determined experimentally was 8.0, differing from that obtained by titration (6.4), which indicated the presence of fixed positive charges in disubstituted imidazole units. The XPS N 1*s* signal for pyridinic nitrogen in the imidazole units, and the O 1*s* signals from the carbonyl, hydroxyl and carboxylate groups shifted to higher binding energies after copper uptake, proving the chemical nature of Cu(II) adsorption on the polyampholyte. The XPS spectrum of the complex showed a Cu $2p_{3/2}$ peak at 934.7 eV and the characteristic shake-up satellite of Cu(II). When the complex was used as a heterogeneous catalyst for H_2O_2 activation, Cu(I) was proved to be a probable intermediate species and contributed to elucidate the mechanism. The Auger CuLMM spectrum supports the presence of Cu(I) with a kinetic energy value of 914.8 eV. The complex was applied in the oxidation of chlorinated phenols in aqueous solution at room temperature without any loss in efficiency.

1. Introduction

Polyampholytes are polymers with anionic and cationic groups located in different monomer units. There are different subclasses of polyampholytes based on their responses to changes in pH, where the anionic and/or cationic groups may be neutralized and/or may be insensitive to changes in pH [1,2].

Recently, a polyampholyte (poly(EGDE-MAA-IM)) derived from methacrylic acid (MAA), imidazole (IM) and ethyleneglycol diglycidyl ether (EGDE) was synthesized by means of a novel one-step synthesis strategy that combines the opening of the epoxy group and a radical polymerization with interesting copper ion uptake (67 mg of Cu(II) ion per gram of polymer) [3,4]. In the Cu(II)–poly(EGDE-MAA-IM) complexes, a competence for the complexation through imidazole and MAA occurs; then, when the imidazole is saturated, the complexation takes place preferentially through MAA, as concluded from previous FTIR and solid-state NMR results [5]. The material bears positive charges from protonated imidazoles and negative charges from carboxylate units, both dependent on pH and determined by titration. Besides, we have previously postulated the presence of disubstituted imidazole residues which should bring fixed positive charges to the polymer network. In this work, the experimental determination of the isoelectric point by zeta potential measurements [6,7] contributed to demonstrate this particular feature, since this value differed from the information obtained by acid–base titration.

X-ray photoelectron spectroscopy (XPS) is a powerful surface analytical technique to assess the chemical composition of macromolecules, ligands and mixedvalent complexes because the oxidation state of the elements can be accurately determined [8–11]. In this work, XPS provided additional evidence on the chemical structure of the polyampholyte described and the mechanism of copper adsorption. Particularly, the complex between this polyampholyte and Cu(II) has been used successfully as a heterogeneous catalyst for hydrogen peroxide activation and decoloration of an azo-dye [12]. The hydrogen peroxide acts as a free-radical initiator by providing hydroxyl radicals that promote the degradation of organics in waste water treatment; in addition, it does not form

* Corresponding author. Tel.: +34 95 2131873; fax: +34 95 2132000.
** Corresponding author. Tel.: +54 11 49648263; fax: +54 11 49648263.
E-mail addresses: castellon@uma.es (E. Rodríguez-Castellón), vcdall@ffyb.uba.ar (V. Campo Dall' Orto).

1381-1169/$ – see front matter © 2011 Elsevier B.V. All rights reserved.
doi:10.1016/j.molcata.2011.02.010

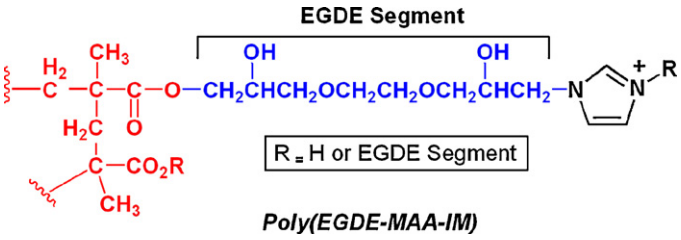

Scheme 1. Representative chemical structure of the polyampholyte.

any harmful by-products, and it is a non-toxic and ecological reactant [13]. However, to enhance the activation, the use of a catalytic system is required [14].

In our system, the most probable mechanism of catalysis (involving the formation of hydroxyl radicals, water and molecular oxygen as products, and Cu(I) as intermediate species) was confirmed by XPS. Finally, the catalyst was tested in the oxidation of chlorinated phenols, which constitute an important class of accumulative highly toxic pollutants.

2. Experimental

2.1. Materials

The polyampholyte was synthesized in a one-step synthetic strategy according to previous reports [3,4], from methacrylic acid (MAA), ethylene glycol diglycidyl ether (EGDE) and imidazole (IM). Then, it was washed with water, dried at 60 °C for 24 h and milled in particles with an average diameter of 200 μm. Scheme 1 exhibits the most representative chemical structure of this product. Three parallel reactions take place in this polymer material: radical polymerization of MAA, which gives a linear polymer (like PMAA), condensation between EGDE and MAA monomers, and reaction of some epoxy-units with imidazole, which results in N-substituted imidazole units or N,N-disubstituted imidazoles. Furthermore, PMAA segments react with imidazole moieties of the EGDE-IM fragments giving some kind of interpolymeric complex, which results in an interesting system with interpenetration of linear and cross-linked polymers [3,4].

Cu(II)–poly(EGDE-MAA-IM) was prepared with 0.100 g of polyampholyte and 2.0 mL of 0.080 M $CuSO_4$ solution in deionised water. Then the sample was centrifuged, washed with deionised water and filtered after 48 h of contact time at 20 °C [4]. The corresponding adsorption isotherm was obtained using $CuSO_4$ solution in a 4–100 mM concentration range.

Methanolic solutions of 119.0 ppb 2,4-dichlorophenol and 108.2 ppb 2,4,5-trichlorophenol were provided by Prof. H. Vélez from INTI. Solvents for chromatographic separation were HPLC grade. The other reagents were of analytical grade.

2.2. Physical measurements

Zeta (ζ) potential (ZP) measurements were performed with a Zeta Potential Analyzer ZetaPlus from Brokhaven Instruments Corporation at 25 °C and constant ionic strength of 10^{-3} M KCl. The polyampholyte suspension (0.25 g/L) was dispersed and shaken on a magnetic stirrer. The pH was adjusted using KOH or HCl and the pH of the final supernatant was measured before and after the ZP measurements. The optical unit contains 35 mW solid state laser red (660 nm wavelength). ZP was measuring using a 16 V cm^{-1} of electric field, 15 mA current and 21 count times.

X-ray photoelectron spectra were collected using a Physical Electronics PHI 5700 spectrometer with non monochromatic Mg Kα radiation (300 W, 15 kV, 1253.6 eV) for the analysis of the core level signals of C 1*s*, N 1*s*, O 1*s*, S 2*p* and Cu 2*p* and with a multichannel detector. Powdered samples were pressed in a sample holder and then introduced in the preparation chamber and evacuated during one night at 10^{-7} Pa. Spectra of powdered samples were recorded with the constant pass energy values at 29.35 eV, using a 720 μm diameter analysis area. During data processing of the XPS spectra, binding energy values were referenced to the C 1*s* peak (284.8 eV) from the adventitious contamination layer. The applied shift for correcting the charging effect was between 2.8 and 3.5 eV [15]. The PHI ACCESS ESCA-V6.0 F software package was used for acquisition and data analysis. A Shirley-type background was subtracted from the signals. Recorded spectra were always fitted using Gaussian–Lorentzian curves, in order to determine the binding energy of the different element core levels more accurately. The error in BE was estimated to be *ca.* 0.1 eV. A short acquisition time of 10 min was used to examine C 1*s*, Cu 2*p* and Cu LMM XPS regions in order to avoid, as much as possible, photoreduction of Cu^{2+} species. Nevertheless, a Cu^{2+} reduction in high vacuum during the analysis cannot be excluded [16]. The used sensitivity factors for the studied elements were C 1*s* (0.314), N 1*s* (0.499), O 1*s* (0.733), S 2*p* (0.717) and Cu 2*p* (4.395).

The FTIR spectra of the polymers and their copper complexes were recorded on a Spectrum 1000 PerkinElmer spectrometer using KBr pellets. The material was dried and placed in a desiccator at 20 °C prior to pellet preparation.

2.3. Catalysis procedures

Cu(II)–poly(EGDE-MAA-IM) was tested as a heterogeneous catalyst for H_2O_2 activation and the degradation of methyl orange (MO), an azo dye, in 0.1 M phosphate buffer at pH 7.0. A 50.0 mL-aliquot of a solution containing the dye and H_2O_2 was put in contact with 50.0 mg of the catalyst. The initial concentrations of H_2O_2 and MO were 50 mM and 40 μM, respectively [12]. After 3 h of reaction, the catalyst was separated from the solution, washed with deionized water, dried at room temperature and placed in a desiccator for further XPS studies.

The Cu(II)–poly(EGDE-MAA-IM) complex was reused in 6 consecutive experiments of decoloration in order to verify the catalytic activity. In this case a 25.0 mL-aliquot of a solution containing the dye and H_2O_2 was put in contact with 50.0 mg of the catalyst. The initial concentrations of H_2O_2 and MO were 40 mM and 10 μM, respectively. After 60 min of reaction, the catalyst was separated from the solution, washed with deionized water and reused in the next experiment. The procedure was made in duplicate, with a new aliquot of catalyst. An adsorption control was made in absence of hydrogen peroxide.

The complex was also tested as a heterogeneous catalyst for H_2O_2 activation and the degradation of 2,4-dichlorophenol (2,4-DCP) and 2,4,5-trichlorophenol (2,4,5-TCP). The working solutions contained: (a) 39.7 μg L^{-1} 2,4 DCP and 0.010 M hydrogen peroxide in deionized water, with an addition of 0.0063 M H_2O_2 at 63 min; and (b) 36.1 μg L^{-1} 2,4,5 TCP and 0.100 M hydrogen peroxide in deionized water. Then 50 mg of the catalyst Cu(I,II)–poly(EGDE-MAA-IM) were suspended in a 15-mL aliquot of each solution and stirred to ensure good mixing. Samples of 0.2 mL were periodically extracted from the reactor using a pipe, and immediately analyzed after they had been filtered through a 0.45 μm-pore diameter syringe filter to remove the particles. The extracted volume was replaced by deionized water and corrections for dilution were made. The concentration of each phenolic compound was monitored by a HPLC system with an amperometric detector placed at +1.0 V vs Ag/AgCl. The column was SGE octyl 5 μm (150 mm × 4 mm), and the mobile phase was acetonitrile:water 50:50 with 0.050 M $LiClO_4$ as supporting electrolyte, at a flow rate of 0.8 mL min^{-1}. Chemical calibration was made before the

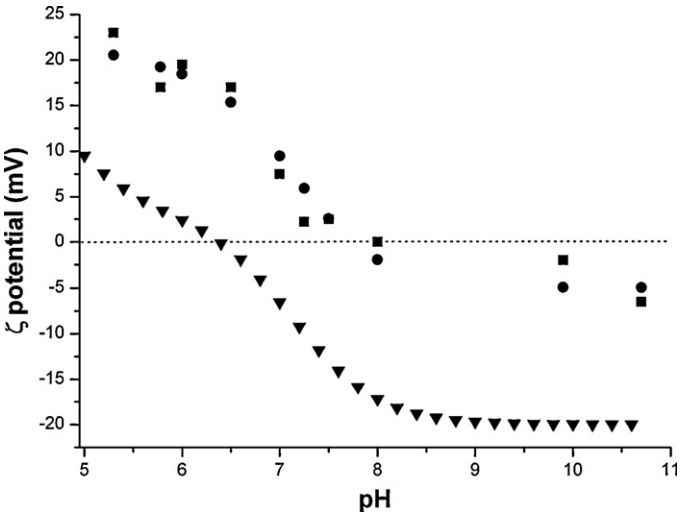

Fig. 1. Effect of pH on the ζ potential of the polyampholyte (■); simulated curve from Eq. (1) and Ra/b: 0.87 (▼); simulated curve from Eq. (1) and Ra/b: 0.2 (●).

analysis of the samples. All the experiments were performed at 20.0 ± 0.5 °C.

3. Results and discussion

3.1. Isoelectric point by measurements of the ζ potential

The zeta (ζ) potential of the polyampholyte particles was measured between pH 5.3 and 10.75 at 25 °C. The relationship between the ζ potential value and the pH value is shown in Fig. 1 (■). The maximum positive and negative ζ potentials were 23 mV at pH 5.3 and −6.5 mV at pH 10.7, respectively. The ζ potentials as a function of pH indicated a sigmoid curve with an isoelectric point at pH 8.0. Namely, the amphoteric particle bears a positive charge between pH 5.5 and 8.0, and a negative charge above pH 8.0. This particle has carboxylate groups, monosubstituted imidazole residues with pyrrolic and pyridinic nitrogen atoms, and a certain number of disubstituted residues, in agreement with solid-state NMR and FTIR evidence [4,5]. Under acidic conditions, the pyridinic nitrogens are protonated, while the carboxyl groups are neutral, leading to an enhancement of the positive ζ potential. Under alkaline conditions, on the contrary, the negative charge increased with pH owing to the deprotonation of carboxyl groups with the pyridinic nitrogen atoms being in a neutral form. Besides, the disubstituted imidazole units bear a positive permanent charge.

This polyampholyte was brought to the acid form and titrated with NaOH. The pK values of the carboxylic group (–COOH) and protonated imidazole residues (IMH^+) were estimated as 4.7 and 7.14, respectively [4]. If the number of disubstituted imidazole groups were negligible, an isoelectric point of 6.0 could be derived from this experiment, taking only the pH-dependent charges into account. In the same sense, using the carboxylic/protonable imidazole ratio resulting from this titration (Ra/b: 0.87) and the estimated pK [4], we obtained an isoelectric point of 6.4 from the simulated curve given by Eq. (1) (Fig. 1, ▼):

$$\zeta = C \times \left[\left(\frac{b \times 10^{-\mathrm{pH}}}{10^{-\mathrm{pH}} + 10^{-\mathrm{pKb}}} \right) - \left(\frac{a \times 10^{-\mathrm{pK}_a}}{10^{-\mathrm{pH}} + 10^{-\mathrm{pK}_a}} \right) \right] \quad (1)$$

where a is the stoichiometric coefficient for the ratio between the carboxylate anion and the total concentration of the carboxyl group, pK_a the negative logarithm of the proton dissociation constant of –COOH, b the stoichiometric coefficient for the ratio between the concentration of the protonated imidazole cation and the total concentration of the imidazole group, pK_b the negative logarithm of the proton dissociation constant of imidazolium and C a proportional constant.

Table 1
Amounts of imidazole and carboxylate groups at pH 8.0 inferred from titration and measurement of the ζ potential.

Site	mmol per gram of polyampholyte	%
Protonated imidazole at pH 8.0	0.16	7
Non-protonated imidazole at pH 8.0	1.14	51
Disubstituted imidazole	0.94	42
Total imidazole	2.24	100
Carboxylate at pH 8.0	1.1	

This value is far from 8.0, which was determined by means of ζ potential measurements (Fig. 1, ■). The experimental data fitted Eq. (1) using pK values of 4.7 and 7.14 (Fig. 1, ●). The isoelectric point derived from this graph was close to 8 but the carboxylic/protonable imidazole ratio was estimated as 0.2, which is not consistent with the elemental analysis and titration results previously reported [4] because the ratio between carboxylic and total imidazole is 0.49.

This provides additional evidence that fixed positive charges from disubstituted imidazoles are present, for which the real isoelectric point must be 8.0 instead of 6.0. Since the pK of imidazole residues is 7.14, at pH 8.0 an 88% of the protonable imidazole has been neutralized. At this point, when most of the positive charge from H^+ has been neutralized, the amount of positive charge in the polymer equals the negative charge from the carboxylate. This can be explained only by the fixed positive charges from the disubstituted imidazole units. Table 1 shows the information inferred from titration and measurement of the ζ potential.

3.2. XPS analysis of poly(EGDE-MAA-IM)

Since the BE of a core-level electron depends on its chemical environment within the molecules, the XPS spectrum provides information on the type and number of different species of a given atom in the molecules.

Fig. 2 exhibits the core level N 1*s* spectrum of native poly(EGDE-MAA-IM) fitted with two distinct peaks at 398.7 eV (47%) and 400.9 eV (53%). Table 2 shows the XPS binding energies and the proportion of the different types of atoms for the elements C, N and O. Here, the two nitrogen atoms in the imidazole residue have different chemical surroundings. The first peak is interpreted as arising from the pyridinic nitrogen-type. The second peak is mainly

Table 2
Data of the XPS spectra of the polyampholyte and its complexes (binding energy and percentage).

C 1*s*	O 1*s*	N 1*s*
Poly(EGDE-MAA-IM)		
284.3 eV (38%)	530.1 eV (13%)	398.7 eV (47%)
285.9 eV (58%)	532.1 eV (87%)	400.9 eV (53%)
288.0 eV (4%)		
Poly(EGDE-MAA-IMH$^+$)		
284.4 eV (12%)	529.8 eV (6%)	400.5 eV (56%)
285.8 eV (31%)	531.4 eV (14%)	402.4 eV (44%)
287.3 eV (50%)	533.5 eV (80%)	
289.2 eV (7%)		
Cu(II)–poly(EGDE-MAA-IM)		
284.8 eV (23%)	530.8 eV (12%)	399.4 eV (30%)
286.3 eV (72%)	532.7 eV (88%)	401.1 eV (70%)
288.6 eV (5%)		
Cu(II)–poly(EGDE-MAA-IM) treated with H_2O_2		
285.4 eV (56%)	531.2 eV (7%)	400.1 eV (56%)
286.9 eV (36%)	533.1 eV (93%)	401.8 eV (44%)
289.0 eV (8%)		

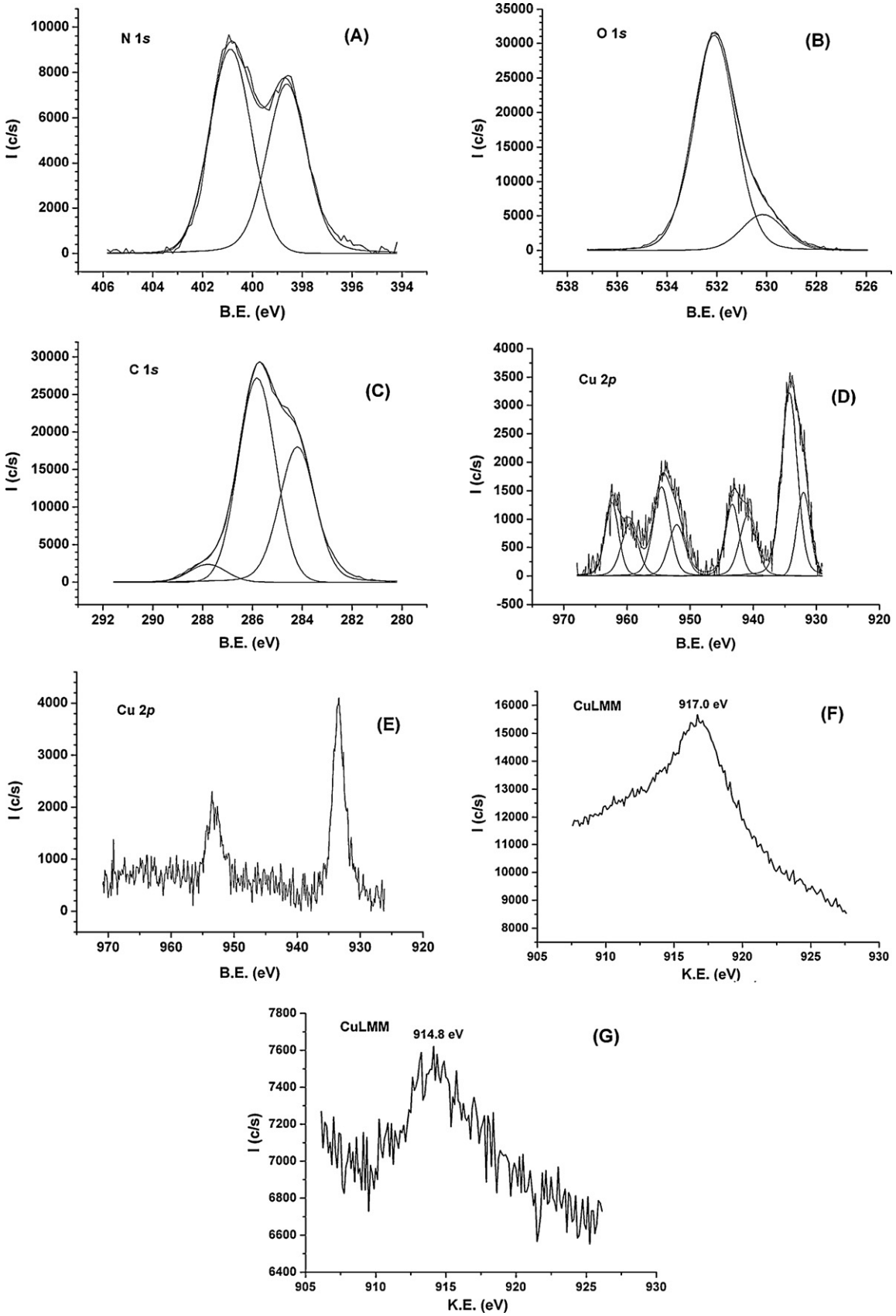

Fig. 2. XPS spectra of the polyampholyte and the copper complexes. The close-up N 1*s* (A); the close-up O 1*s* (B); the close-up C 1*s* (C); the close-up Cu 2*p* in the complex (D); the close-up Cu 2*p* in the complex after treatment with H_2O_2 (E). Auger CuLMM spectra of the polyampholyte–copper complexes before (F) and after treatment with H_2O_2 (G).

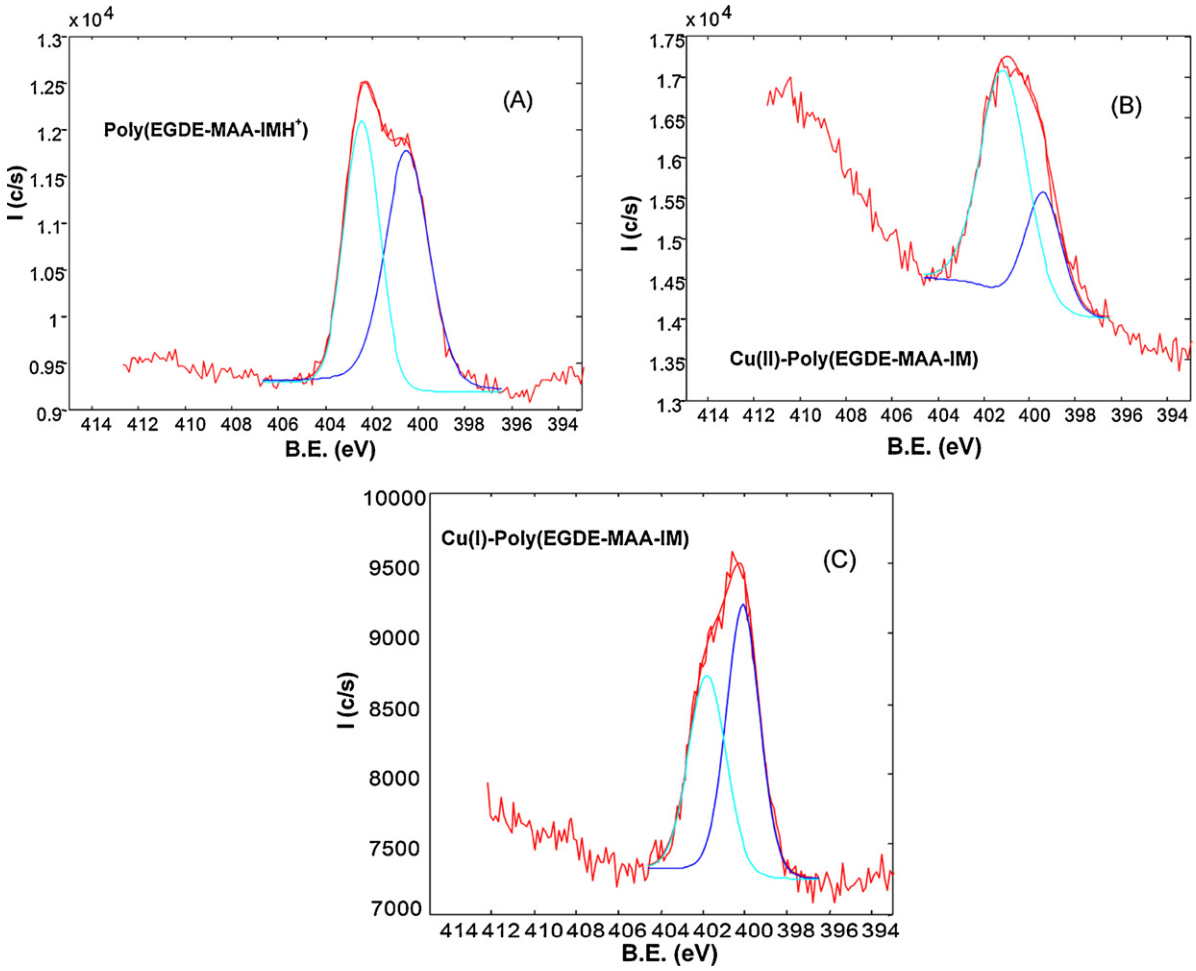

Fig. 3. The close-up N 1*s* of the polyampholyte treated with HCl (A); the Cu(II)-complex (B) and the Cu(I) complex (C).

attributed to the pyrrolic nitrogen-type through which the imidazole ring is attached to the main chain. This assignment is based on the consideration that the lone pair of electrons of the pyrrolic nitrogen-type is involved in π-system, and that thus the electronic environment of this nitrogen is more electron-deficient than that of the pyridinic nitrogen-type, leading to a higher BE [17].

The peak centered at 400.9 eV should also include the signals of a small amount of protonated nitrogen and the nitrogen from disubstituted imidazole units.

In disubstituted rings there is a delocalization of the positive charge across the cation and the two nitrogen atoms should behave as equivalents, in this case with a BE of *ca*. 401 eV as found in ionic liquids [18,19].

From these results, it can be inferred that 94% of the imidazole units are monosubstituted and non-protonated, and that the remaining 6% includes disubstituted rings and protonated imidazoles. For the native polyampholyte, the amount of protonated imidazole residues is expected to be 7% or less.

There was no match between the number of disubstituted units obtained from the combination of elemental analysis with titration (43%) [4] and that obtained from these last results. However, the results from XPS correspond to the exposed surface of the particle and do not exhibit the bulk or pore structure.

Fig. 3A also exhibits the data of the N 1*s* spectrum for the fully protonated polyampholyte (treated with 1 M HCl aqueous solution) (Table 2). In this case, the spectrum was curve-fitted into two peaks. The component at 400.5 eV (56%) could be associated with the pyrrolic nitrogen-type and possibly with disubstituted imidazoles. The binding energy around 402–403 eV is generally found in positive nitrogen atoms from ammonia, polyaniline and other similar examples [20,21]. The possibility of an N-oxide [22,23] was discarded because the FTIR signals at 1210 and 830 cm^{-1}, consistent with this functionality, were absent (Fig. 4) [24,25]. In this case, we assigned the component at 402.4 eV (44%) to the protonated

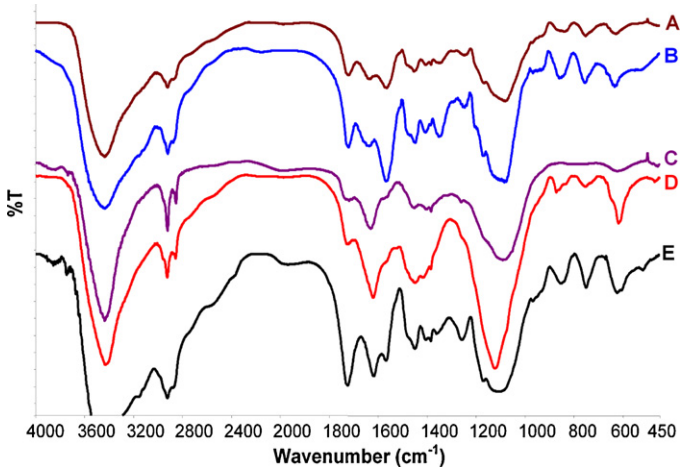

Fig. 4. FTIR spectra of poly(EGDE-MAA-IM) (A); poly(EGDE-MAA-IM) treated with NaOH (B); poly(EGDE-MAA-IMH+) (C); Cu(II)–poly(EGDE-MAA-IM) (D); Cu(II)–poly(EGDE-MAA-IM) treated with H_2O_2 (E).

pyridine nitrogen-type. Again, monosubstituted rings are predominant in this material, in a proportion of 88%. Several authors have determined that when the N of pyridine, piperidine or imidazole is protonated, the BE value of N 1*s* is increased by 2.0 eV or more. On the other hand, if the N is involved in hydrogen bonding interaction, the BE is increased by less than 1.0 eV [17,26]. In our experiment, the protonation of the imidazole units caused a core-level chemical shift of 3.7 eV to higher binding energy in N 1*s* associated with the decrease in electron density.

3.3. Study of the mechanism of copper adsorption

The equilibrium of Cu(II) adsorption to the surface of the polyampholyte was studied [4]. The experimental data at 20 °C fitted to Langmuir isotherm, with an estimated K_d of 5×10^{-3} M^{-1} (SD: 1×10^{-3}) and a maximum loading capacity of 67 mg of Cu(II) per gram of polyampholyte (SD: 4). Then the heterogeneous catalyst was prepared under conditions of saturation with Cu(II).

To further elucidate the mechanism of copper ion adsorption on the polyampholyte particles, XPS analysis was conducted both before and after copper ion adsorption. The reaction of the material with Cu(II) gives a blue-green Cu(II)–polyampholyte complex. Upon the addition of Cu(II) solution to a suspension of this polymer, the pH of the medium decreased from 8.0 to 5.5. This suggests that the sorption process involves the exchange of copper ions with protons, and that, at the same time, the weak groups that did not bind copper might be acting as pH buffers. The study was then oriented to understand if there was an ion exchange process or if two chemical equilibria (complexation and acid–base) were competing.

The N 1*s* spectrum was fitted using two Gaussian–Lorentzian peaks with energies of 399.4 (30%) and 401.1 eV (70%), respectively (Fig. 3B and Table 2). The first peak was assigned to the pyridinic nitrogen coordinated with copper ion, whereas the second one was assigned to the pyrrolic nitrogen (at *ca.* 400.5 eV) and the disubstituted imidazole groups. Comparing the N 1*s* spectrum of the polyampholyte with the spectrum of the complex with copper ion, we observed a significant shift of the binding energy of the first peak (398.7–399.4 eV) (Figs. 2A and 3B). The increase in the BE provides evidence that the pyridinic nitrogen was involved in the adsorption of the copper ions. Here the lone pair electrons from the nitrogen atoms were shared with the copper ions, increasing the oxidation state and thus the BE of the nitrogen atoms involved. It was also noted that the area under the peak at 401.1 eV was increased, compared with the spectrum of the non-complexed polyampholyte. We attribute this to the protonation of non-complexed pyridinic nitrogen-type atoms at pH 5.5.

Strong evidence of coordination was found in FTIR spectra (Fig. 4). The absorption intensity at 1650 cm^{-1} related to imidazole ring stretching was significantly improved after copper uptake. The broad asymmetric band at *ca.* 620 cm^{-1} in the complex was assigned to the stretching vibration of the Cu(II)–N bond [9] and to the stretching vibration of S–O (expected at 600 cm^{-1}) from the $CuSO_4$ salt used in the binding experiments [10]. In addition, the presence of sulphur found in previous SEM-EDS results was also observed [4]. The last contribution increased with the amount of copper ion, which indicates that SO_4^{2-} exists at least as an ion pair in the complex, probably as a counterion of copper itself or of disubstituted imidazole residues. The S 2*p* spectrum was asymmetric and was associated with the doublet S $2p_{3/2}$ and S $2p_{1/2}$ at 168.9 and 170.4 eV, respectively, and was attributed to SO_4^{2-} (Table 3).

The XPS investigation of the Cu(II)–poly(EGDE-MAA-IM) complex at the Cu 2*p* level showed a broad Cu $2p_{3/2}$ signal that can be decomposed into two contributions at 932.5 eV (26%) and 934.7 eV (74%) (Fig. 2) and the corresponding shake-up satellite peaks. Moreover, the intensity ratio of the shake-up satellite and the intensity of the Cu $2p_{3/2}$ peak (ICu_{sat}/ICu_{2p}) was 0.50, a value close to that found for CuO (0.55) [27]. The contribution at a higher binding energy (934.7 eV) and the observed ICu_{sat}/ICu_{2p} ratio indicate that most of copper is as Cu(II). The contribution at 932.5 was assigned to reduced copper species, probably Cu(I). The study of the CuLMM signal also supports the presence of Cu(I). In Fig. 2F the Auger CuLMM signal shows a maximum of the kinetic energy at 917.0 eV assigned to Cu(II) and a shoulder at 914.9 eV due to the presence of reduced copper (Table 3) [28].

Table 3
Data of the XPS spectra of the copper complexes (binding energy (in eV) for S $2p_{3/2}$ and Cu $2p_{3/2}$ and kinetic energy (also in eV) for CuLMM).

S $2p_{3/2}$	Cu $2p_{3/2}$	CuLMM
Cu(II)–poly(EGDE-MAA-IM)		
168.9 eV (69%)	932.5 eV (26%)	914.9 (shoulder)
170.4 eV (31%)	934.7 eV (74%)	917.0
Cu(II)–poly(EGDE-MAA-IM) treated with H_2O_2		
–	933.4 eV (95%)	914.8
–	935.3 eV (5%)	

The deconvolution of the O 1*s* peak yielded two contributions (Fig. 2 and Table 2). The peaks at 530.1 and 530.8 eV (before and after Cu(II) adsorption) were attributable to the C=O group [29,30], whereas the peaks at 532.1 eV (observed before Cu(II) adsorption) and 532.7 eV (observed after Cu(II) adsorption) were attributable to the C–O (carbons from EGDE moieties) and $–COO^-$ groups. The shift of the oxygen signals to higher binding energies after Cu(II) adsorption was probably caused by the binding of copper ions onto the oxygen atoms, which reduced their electron density. The relative content of oxygen in the second peak was slightly increased probably due to the contribution of SO_4^{2-} expected at about 532 eV.

The peaks at 284.3 and 284.8 eV (before and after Cu(II) adsorption) were attributable to adventitious carbon and to carbon atoms from the imidazole groups (Fig. 2 and Table 2), the peaks at 285.9 and 286.3 eV (observed before and after Cu(II) adsorption) to aliphatic carbon and to the C–O functionalities (carbons from EGDE moieties), and those at 288.0 and 288.6 eV (observed before and after Cu(II) adsorption) to C=O and to $–COO^-$ groups [15,30]. The FTIR spectrum presented in a previous work [4,5] (Fig. 4) exhibited a sharp decrease in the intensity of the asymmetric stretching band of $–COO^-$ at 1570 cm^{-1} after copper ion adsorption at high concentrations of Cu(II) in solution. Besides, the stretching vibrations of C–O at 1100 cm^{-1} corresponding to hydroxyl and ether groups shifted to higher wavenumbers.

Evidently, nitrogen, oxygen and carbon atoms are inclined to transfer the electron pair. This implies that the imidazole group, as well as the hydroxyl and $–COO^-$ groups are involved in the coordination of Cu(II) during the adsorption process in a different magnitude as was also observed in previous solid-state NMR experiments [5]. Moreover, previous thermogravimetric studies in this Cu(II)-complex have shown that the thermal stability in this complex is affected by changes in the electronic density in the polymer matrix associated with the metal ion [5].

The treatment of the polyampholyte with HCl gave a different profile. The signal at 533.5 eV could be assigned to the O from ether and hydroxyl groups, not affected by changes in pH. Instead, the peaks at 529.8 (6%) and 531.4 eV (14%), attributed to C=O and –COOH, respectively, were shifted to a lower BE in acidic medium. For carbon, a peak at 287.3 eV was attributed to the C=O group, and a variation in the BE between $–COO^-$ (288 eV) and –COOH (289.2 eV) was found to be due to a decrease in electron density occurred after protonation [30]. The absorption intensity at 1650 cm^{-1} related to imidazole ring stretching was significantly improved after proton uptake, and there was a sharp decrease in the intensity of the $–COO^-$ signal at 1570 cm^{-1} (Fig. 4).

3.4. Analysis of the mechanism of catalysis by XPS

Cu(II)–polyampholytes and other derivatives have been used as heterogeneous catalysts for hydrogen peroxide activation and degradation of methyl orange, an azo-dye [12].

The catalytic properties of Cu(II)–poly(EGDE-MAA-IM) were confirmed by recycling the complex in six consecutive experiments of methyl orange decolorization. In the first five batches of degradation, the decolorization took place in less than 60 min. The reaction rates were lower in the sixth cycle possibly due to a partial loss of catalyst in the washing stage.

In particular, the Cu(II)–poly(EGDE-MAA-IM) treated with H_2O_2 used in this work presented several remarkable changes in the XPS spectrum. For N 1*s* all the signals shifted to a higher BE and now there is a parallelism between the N 1*s* lines for the complex treated with H_2O_2 and for the polyampholyte treated with HCl (poly(EGDE-MAA-IMH$^+$)) (Fig. 3 and Table 2).

In this case, we expected 44% of pirrolic nitrogen-type at 400.1 eV, 44% of Cu–N at 401.8 eV (a percentage higher than that before the treatment with H_2O_2 probably due to some type of structural rearrangement on the surface of the material) and about 12% of disubstituted imidazole at *ca*. 401 eV. The Cu $2p_{3/2}$ appeared at 933.4 eV. This BE value, together with the absence of shake-up satellite peaks, is consistent with the presence of reduced copper species, more probably Cu(I) [9,31]. The Auger CuLMM spectrum (Fig. 2G) strongly supports the presence of Cu(I) with a kinetic energy value of 914.8 eV. A very small amount of Cu(II) could be assigned from the weak shoulder at 935.3 eV in the XPS spectrum of Fig. 2E (Table 3).

The presence of Cu(I) after treatment with H_2O_2 is indicative of a mechanism of peroxide decomposition that involves Cu(I) as intermediate according with [32]:

$$\begin{array}{rcl} \text{L-Cu}^{2+} + \text{H}_2\text{O}_2 & \longrightarrow & \text{L-Cu}^{+\bullet}\text{O}_2\text{H} + \text{H}^+ \\ \text{L-Cu}^{+\bullet}\text{O}_2\text{H} + \text{H}_2\text{O}_2 & \longrightarrow & \text{L-Cu}^{+} + \text{O}_2 + {}^{\bullet}\text{OH} + \text{H}_2\text{O} \\ \text{L-Cu}^{+} + \text{H}_2\text{O}_2 & \longrightarrow & \text{L-Cu}^{2+} + {}^{\bullet}\text{OH} + \text{OH}^- \\ \hline 3\ \text{H}_2\text{O}_2 & \longrightarrow & \text{O}_2 + 2\ {}^{\bullet}\text{OH} + 2\ \text{H}_2\text{O} \end{array}$$

In fact, when H_2O_2 is added to the solution, bubbles of gas are formed and hydroxyl radical is detected by ESR [12].

The XPS measurements were made on samples treated with H_2O_2 after a relatively long contact period in which the peroxide was consumed. In this condition of H_2O_2 depletion, the slowest stage of this catalytic cycle would determine the final form of the catalyst in the analyzed sample. According with XPS and Auger results, the conversion of L-Cu$^+$ to L-Cu^{2+} should be the slowest step, so that L-Cu$^+$ would accumulate on H_2O_2 consumption. In other words, after the first cycle the catalytic mechanism could be written as:

$$\begin{array}{rcl} \text{L-Cu}^{+} + \text{H}_2\text{O}_2 & \longrightarrow & \text{L-Cu}^{2+} + {}^{\bullet}\text{OH} + \text{OH}^- \\ \text{L-Cu}^{2+} + \text{H}_2\text{O}_2 & \longrightarrow & \text{L-Cu}^{+\bullet}\text{O}_2\text{H} + \text{H}^+ \\ \text{L-Cu}^{+\bullet}\text{O}_2\text{H} + \text{H}_2\text{O}_2 & \longrightarrow & \text{L-Cu}^{+} + \text{O}_2 + {}^{\bullet}\text{OH} + \text{H}_2\text{O} \\ \hline 3\ \text{H}_2\text{O}_2 & \longrightarrow & \text{O}_2 + 2\ {}^{\bullet}\text{OH} + 2\ \text{H}_2\text{O} \end{array}$$

With this last XPS evidence, the decomposition mechanism is confirmed.

The core level O 1*s* signal of the Cu(I,II) complex was decomposed in two contributions at 531.2 eV (7%) and 533.1 eV (93%) eV. The first contribution might be assigned to the oxygen atom of the C=O group and the second to the oxygen in the –COO$^-$, –OH and C–O–C groups [29,30]. These signals were shifted from the spectrum of the polyampholyte without copper as well as from the spectrum of the polyampholyte with Cu(II) (Table 2). All shifts occurred towards a higher BE, which indicates that all the groups are involved in the charge transfer from the ligands to Cu(I) in coordinated bonds. The XPS investigation showed the binding energies for C 1*s* in the Cu(I,II) complex. The three peak components showed significant changes compared with those of the polyampholyte and the complex with Cu(II) (Table 2). Again, shifts towards a higher BE are indicative of lower electron density of all the C atoms bound to oxygen or nitrogen.

From these results, it can be concluded that electron transfer also exists between the oxygen, carbon and nitrogen atoms and Cu(I), and that there is coordination between the polyampholyte and Cu(I) ions.

In particular, the Cu(I)-complex obtained may be interesting because a variety of Cu(I) sources are known to catalyze the cyclopropanation reaction [33] and cycloadditions of organic azides and alkynes [34]. Moreover, a modified alumina supported copper nanoparticles and a silica immobilized copper complexes were used as catalyst in the synthesis of 1,2,3-triazoles and N-arylation of heterocycles and benzylamines [35,36].

The FTIR spectrum of this catalyst resembles the spectrum of the polyampholyte previously treated with NaOH, except for the decrease in the intensity of the asymmetric stretching band of –COO$^-$ at 1570 cm^{-1} and for a broader band at 620 cm^{-1} corresponding to the stretching vibration of the Cu–N bond (Fig. 4). These results confirm the presence of the metal ion but do not provide information about the oxidation state.

When the Cu(II)–poly(EGDE-MAA-IM) was treated with hydrogen peroxide, the XPS signal of sulphur was lost and the FTIR signal at 600 cm^{-1} was weaker. This could be attributed to the release of the counterion SO_4^{2-} due to the reduction of Cu(II) to Cu(I). The remaining positive charge would be now balanced by carboxylate and chloride.

3.5. Degradation of chlorinated phenols by catalytic activation of H_2O_2

Wet peroxide oxidation processes using H_2O_2 as the oxidant are considered acceptable alternative technologies for the destruction of pollutants [13]. Although chlorinated phenols have been reported to be degraded by bacteria or plants, long reactor residence times are often required [37]. Some physical and chemical methods including adsorption over activated carbon, air stripping, solvent extraction, ultraviolet light and ozone, with limitations because of the high cost and low efficiency, have also been used for the removal of CPs and their derivatives from wastewater [38]. In this work, we evaluated the performance of this recoverable heterogeneous catalyst combined with a clean oxidant.

Fig. 5 plots the CPs concentrations against the time under various conditions. The overall process of CP removal from the solution was expected to involve surface adsorption and oxidative degradation. Both adsorbed and soluble CP molecules can be oxidized by the free radicals formed from H_2O_2 [12]. The most probable products were chlorinated o-benzoquinones, which were not expected to be amperometrically detected at +1 V by the HPLC system.

For 2,4-DCP in contact with the catalyst and without H_2O_2, the concentration of the phenol barely declined, indicating that the adsorption to the complex is less than 10%.

The reaction rate of 2,4-DCP with 0.010 M H_2O_2 was enhanced by the catalyst. The concentration decreased linearly, indicating a saturation in hydrogen peroxide, with a degradation constant of 0.0051 μg L^{-1} s^{-1} (SD: 0.0001; R: 0.9986), and a 46% of decomposition at 60 min. The new addition of the oxidant at 63 min confirmed the zero order for the oxidant. In the absence of the catalyst, there was 21% of degradation after 60 min.

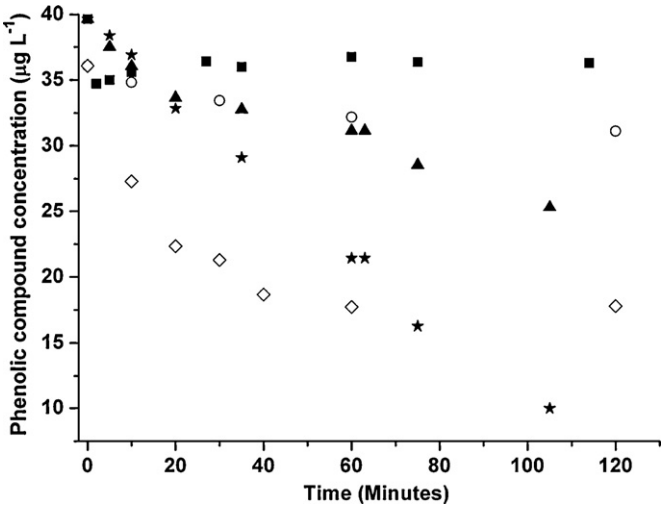

Fig. 5. Phenolic profile under different experimental conditions. For 2,4-DCP: with H_2O_2 (▲), with the catalyst (■), with both H_2O_2 and the catalyst (⋆). For 2,4,5-TCP: with H_2O_2 (○), with both H_2O_2 and the catalyst (◊).

Table 4
Kinetic parameters for 40 μg L^{-1} 2,4,5-TCP degradation with 0.100 M hydrogen peroxide.

Regression parameters	Catalyzed reaction	Non-catalyzed reaction
$[2,4,5\text{-TCP}]_\infty$ (μg L^{-1})	17.6 (SD: 0.4)	30.8 (SD: 0.2)
$[2,4,5\text{-TCP}]_{deg}$ (μg L^{-1})	18.4 (SD: 0.7)	5.2 (SD: 0.2)
k (s^{-1})	1.06×10^{-3} (SD: 9×10^{-5})	3.8×10^{-4} (SD: 3×10^{-5})
R	0.9974	0.9992

For 2,4,5-TCP, the rate of degradation was also enhanced by the catalyst. This compound required 0.100 M of hydrogen peroxide and the reaction proceeded in a less time than for 2,4-DCP. The concentration of 2,4,5-TCP exhibited an exponential decay according to the empirical kinetic expression (2),

$$[2,4,5\text{-TCP}] = [2,4,5\text{-TCP}]_\infty + [2,4,5\text{-TCP}]_{deg} \times e^{-k \times t} \quad (2)$$

where $[2,4,5\text{-TCP}]_\infty$ represents the phenolic compound at equilibrium, $[2,4,5\text{-TCP}]_{deg}$ was the amount decomposed by free radicals, and k is the pseudo-first order kinetic constant. Table 4 summarizes the empirical parameters for the reaction with and without the catalyst, showing a substantial difference. The kinetic constant increased 2.8 times in the presence of this complex. The amount of 2,4,5-TCP at equilibrium could depend on the initial rate of production of •OH: when the reaction was catalyzed a higher concentration of free radicals may be produced at the beginning, leading eventually to a higher percentage of oxidized TCP. The stability of the complex was good for the first case. At 0.100 M of hydrogen peroxide, the complex can be used twice without loss of efficiency.

4. Conclusions

The studies presented in this work provide significant evidence about the chemical structure of the polyampholyte and the Cu(I,II)-complex.

The functional groups attached to the network were carefully identified by means of the spectroscopic techniques. The results of the acid–base titration and the isoelectric point analyzed together indicated the presence of disubstituted imidazole units in the network.

The XPS analysis demonstrated that nitrogen, oxygen and carbon atoms bound to Cu(II) were inclined to transfer the electron pair. The FTIR analysis showed changes in the signals related to acid and basic functional groups. This implies that the imidazole, hydroxyl and –COO$^-$ groups are involved in the coordination of Cu(II).

The treatment with hydrogen peroxide produced a significant reduction of Cu(II) to Cu(I), determined by XPS and Auger experiments, which confirmed the mechanism proposed for the catalytic activation of the substrate.

Cu(I,II)–poly(EGDE-MAA-IM) was tested in the oxidation of chlorinated phenols as model pollutants. The rate of degradation was enhanced and the extension of the reaction was also improved. The system offered the advantages of a recoverable heterogeneous catalyst and a clean substrate.

Acknowledgements

We thank the financial support from Universidad de Buenos Aires (UBACyT 08-10/B058), CONICET, ANPCyT (BID 1728/PICT 01778) and Universidad de Málaga (project MAT2009-10481) and FEDER funds. Juan Manuel Lázaro Martínez and Lisandro Denaday thank CONICET for their doctoral fellowships.

Appendix A. Supplementary data

Supplementary data associated with this article can be found, in the online version, at doi:10.1016/j.molcata.2011.02.010.

References

[1] A.B. Lowe, C. McCormick, Chem. Rev. 102 (2002) 4177–4190.
[2] S. Colak, G.N. Tew, Macromolecules 41 (2008) 8436–8440.
[3] M.F. Leal Denis, R.R. Carballo, A.J. Spiaggi, P.C. Dabas, V. Campo Dall' Orto, J.M. Lázaro Martínez, G.Y. Buldain, React. Funct. Polym. 68 (2008) 169–181.
[4] J.M. Lázaro Martínez, M.F. Leal Denis, V. Campo Dall' Orto, G.Y. Buldain, Eur. Polym. J. 44 (2008) 392–407.
[5] J.M. Lázaro Martínez, A.K. Chattah, G.A. Monti, M.F. Leal Denis, G.Y. Buldain, V. Campo Dall' Orto, Polymer 49 (2008) 5482–5489.
[6] M. Tschapek, R.M. Torres Sánchez, C. Wasowski, Colloid Polym. Sci. 254 (1976) 516–521.
[7] A. Moncho, F. Martínez López, R. Hidalgo Álvarez, Colloids Surf. A 192 (2001) 215–226.
[8] N.H. Turner, J.A. Schreifels, Anal. Chem. 72 (2000) 99–110.
[9] B. Wang, F. Gao, H. Ma, J. Hazard. Mater. 144 (2007) 363–368.
[10] S. Sun, A. Wang, J. Hazard. Mater. 131 (2006) 103–111.
[11] Y.D. Cao, Q.Y. Zheng, C.F. Chen, H.M. Hu, Z.T. Huang, Inorg. Chim. Acta 357 (2004) 316–320.
[12] J.M. Lázaro Martínez, M.F. Leal Denis, L.L. Piehl, E. Rubín de Celis, G.Y. Buldain, V. Campo Dall' Orto, Appl. Catal. B 82 (2008) 273–283.
[13] L.F. Liotta, M. Gruttadauria, G. Di Carlo, G. Perrini, V. Librando, J. Hazard. Mater. 162 (2009) 588–606.
[14] X.H. Li, X.G. Meng, Q.H. Pang, S.D. Liu, J.M. Li, J. Du, C.W. Hu, J. Mol. Catal. A: Chem. 328 (2010) 88–92.
[15] J.F. Moulder, W.F. Stickle, P.E. Sobol, K.D. Bomben, Standard Spectra for Identification and Interpretation of XPS data, Perkin Elmer, Eden Prairie, MN, 1992.
[16] S. Poulston, P.M. Parlett, P. Stone, M. Bowker, Surf. Interf. Anal. 24 (1996) 811–820.
[17] X. Li, S.H. Goh, Y.H. Lai, A.T.S. Wee, Polymer 42 (2001) 5463–5469.
[18] P. Yu, Y. Lin, L. Xiang, L. Su, J. Zhang, L. Mao, Langmuir 21 (2005) 9000–9006.
[19] H. Zhang, H. Cui, Langmuir 25 (2009) 2604–2612.
[20] H.Q. Xie, Q. Xiang, Eur. Polym. J. 36 (2000) 509–517.
[21] C. Combellas, F. Kanoufi, S. Sanjuan, C. Slim, Y. Tran, Langmuir 25 (2009) 5360–5370.
[22] H. Schmiers, J. Friebel, P. Streubel, R. Hesse, R. Kopsel, Carbon 37 (1999) 1965–1978.
[23] K. Stanczyk, R. Dziembaj, Z. Piwowarska, S. Witkowski, Carbon 33 (1995) 1383–1392.
[24] M. Vieites, P. Smircich, L. Guggeri, E. Marchán, A. Gómez Barrio, M. Navarro, B. Garat, D. Gambino, J. Inorg. Biochem. 103 (2009) 1300–1306.
[25] C. Soykan, R. Coskun, A. Delibas, Thermochim. Acta 456 (2007) 152–157.
[26] D. Nolting, N. Ottosson, M. Faubel, I.V. Hertel, B. Winter, J. Am. Chem. Soc. 130 (2008) 8150–8151.
[27] G. Avgouropoulos, T. Ioannides, Appl. Catal. A 244 (2003) 155–167.
[28] E. Basaldella, E. Tara, G. Aguilar Armenta, M.E. Patiño Iglesias, E. Rodríguez Castellón, J. Sol-Gel Sci. Technol. 37 (2006) 141–146.
[29] M. Toupin, D. Belanger, Langmuir 24 (2008) 1910–1917.

[30] J.C. Zheng, H.M. Feng, M.H.W. Lam, P.K.S. Lam, Y.W. Ding, H.Q. Yu, J. Hazard. Mater. 171 (2009) 780–785.
[31] S. Wu, E.T. Kang, K.G. Neoh, Appl. Surf. Sci. 174 (2001) 296–305.
[32] L. Pecci, G. Montefoschi, D. Cavallini, Biochem. Biophys. Res. Commun. 235 (1997) 264–267.
[33] R. Ahuja, A.G. Samuelson, J. Organomet. Chem. 694 (2009) 1153–1160.
[34] P. Li, L. Wang, Y. Zhang, Tetrahedron 64 (2008) 10825–10830.
[35] M. Lakshmi Kantam, V. Swarna Jaya, B. Sreedhar, M. Mohan Rao, B.M. Choudary, J. Mol. Catal. A: Chem. 256 (2006) 273–277.
[36] P.R. Likhar, S. Roy, M. Roy, M. Lakshmi Kantam, R. Lal De, J. Mol. Catal. A: Chem. 271 (2007) 57–62.
[37] S.T. Hu, Y.H. Yu, Ozone: Sci. Eng. 16 (1994) 13–28.
[38] B.W. Zhu, T.T. Lim, J. Feng, Chemosphere 65 (2006) 1137–1146.